View metadata, citation and similar papers at core.ac.uk

brought to you by CORE

provided by VBN

Aalborg Universitet

AALBORG UNIVERSITY
DENMARK

# Autonomous and Decentralized Load Sharing and Energy Management Approach for DC Microgrids

Azizi, Ali; Peyghami, Saeed; Mokhtari, Hossein; Blaabjerg, Frede

*Published in:*
Electric Power Systems Research

*DOI (link to publication from Publisher):*
10.1016/j.epsr.2019.106009

*Publication date:*
2019

*Document Version*
Early version, also known as pre-print

Link to publication from Aalborg University

*Citation for published version (APA):*
Azizi, A., Peyghami, S., Mokhtari, H., & Blaabjerg, F. (2019). Autonomous and Decentralized Load Sharing and Energy Management Approach for DC Microgrids. *Electric Power Systems Research*, *177*, [106009]. https://doi.org/10.1016/j.epsr.2019.106009

**General rights**
Copyright and moral rights for the publications made accessible in the public portal are retained by the authors and/or other copyright owners and it is a condition of accessing publications that users recognise and abide by the legal requirements associated with these rights.

? Users may download and print one copy of any publication from the public portal for the purpose of private study or research.
? You may not further distribute the material or use it for any profit-making activity or commercial gain
? You may freely distribute the URL identifying the publication in the public portal ?

**Take down policy**
If you believe that this document breaches copyright please contact us at vbn@aub.aau.dk providing details, and we will remove access to the work immediately and investigate your claim.

# Autonomous and Decentralized Load Sharing and Energy Management Approach for DC Microgrids

***Abstract:*** **Appropriate power sharing and energy management in DC microgrids for the optimal, reliable and efficient operation of renewable energies and storages are of high importance. Droop-based control methods have been presented for power sharing among DC sources, while the energy management approaches employ communication systems to monitor the demand, renewable generations and energy level of storage units in order to properly operate the energy sources. Employing communication systems may affect the system reliability and introduce infrastructure costs. Moreover, extending energy sources require modifying the energy management system. This paper proposes an autonomous and decentralized power sharing and energy management approach for DC microgrids without utilizing a communication system. Hence, it can be a reliable and economical solution for operation of DC microgrids. Furthermore, in the proposed approach, the energy sources can operate independently by using the local information, and hence, it introduces plug-and-play capability for extending the energy sources. The viability and effectiveness of the proposed approach are evaluated by simulations and validated by experiments.**

***Index Terms*— DC microgrid, energy management, PV array, battery storage, power sharing.**

## NOMENCLATURE

| | |
|---|---|
| *IC* | *Interlinking Converter* |
| *SoC* | *State of Charge* |
| $V_{INV}$ | *Reference Voltage of IC* |
| $V_{oinv}$ | *Output Voltage of IC* |
| $I_{max}$ | *Maximum Current of IC* |
| $I_{Load}$ | *Load Current* |
| $V_{PCC}$ | *Point of Common Coupling (DC BUS) Voltage* |
| $I_{INV}$ | *Current of IC* |
| $V_{ink}$ | *Input Voltage of $k^{th}$ Battery* |
| $V_B$ | *Reference Voltage of Battery* |
| $I_{Bk}$ | *Current of $k^{th}$ Battery* |
| $V_{ok}$ | *Output Voltage of $k^{th}$ Battery* |
| $R_{dk}$ | *Droop Gain of $k^{th}$ Battery* |
| $C_{bk}$ | *Capacity of $k^{th}$ Battery* |
| $C_{bmax}$ | *Capacity of the largest Battery* |
| $I_{Lk}$, $I_{LK}^*$ | *Current and reference current of $k^{th}$ Battery* |
| $V_{PV}$ | *Reference Voltage of PV* |
| $V_{oPV}$ | *Output Voltage of PV* |
| $V_{inPV}$ | *Voltage of PV array* |
| $I_{LPV}$, $I_{LPV}^*$ | *Current and reference current of PV array* |
| $V_{max}$ | *Maximum Allowable Voltage* |
| $V_{min}$ | *Minimum Allowable Voltage* |
| $P_{Load}$ | *Load Power* |
| $V_{abc}$, $I_{abc}$ | *AC Grid three-phase Voltage and Current* |
| $G_{V,INV}$ , $G_{V,PV}$ | *Proportional-Integrator (PI) Regulators* |
| $Kp$,$K_i$ | *Coefficients of PI controller* |
| *ch/dch* | *Charging/Discharging* |
| *X** | *Reference Value for X* |
| $V_{dq}$,$I_{dq}$ | *Grid dq-axis voltages and currents* |
| $I_d^*$,$I_q^*$ | *dq-axis reference currents* |
| $I_{MPPT}$ | *Maximum Power Point Tracking Current of PV* |
| *KCL* | *Kirchhoff Current Law* |

## I. INTRODUCTION

DC microgrid has become a more applicable, efficient and stable technology and a future grid structure to integrate DC sources and loads, such as Photovoltaic(PV) arrays, Fuel Cell (FC) modules, battery storages, motor driven loads, and full-scale converter-based generators [1]. The DC microgrid technology has been employed to supply the power in the distribution systems and data centers as well as in islanded applications

Pre Print

such as space stations [2], aircraft [3], ships [4], [5], remote areas, and etc. [6], [7]. Furthermore, microgrid technologies make an infrastructure for employing renewable resources to be stably operated together with the battery storages. The battery storages are the main component of a microgrid, which support the microgrid demand and form the DC voltage in islanded operation mode [8]–[12]. Therefore, the energy level of batteries requires to be appropriately managed and they should be charged during grid connection and/or a high generation of MPPT units. Furthermore, the charging and discharging procedure may affect the corresponding lifecycle as well as the reliability of the overall system. In order to increase the lifecycle of batteries, an equalizing approach has been presented to keep the State of Charge (SoC) level of batteries to be asymptotic during charging and discharging mode [8]–[12].

Moreover, in grid-connected mode, the DC microgrid can be connected to the utility through an Interlinking Converter (IC) which transfers power from the microgrid to the utility grid and vice-versa [13]–[16]. The IC can regulate the DC voltage and support the microgrid demand. However, it may be limited by the Distribution System Operator (DSO), and hence, the DC sources should support the microgrid if the IC cannot do it [14]–[17]. Therefore, a coordinated power sharing and energy management approach is required in order properly to control the power and energy flow among different sources and storages in the microgrid.

A variety of research works have been performed on power sharing control strategies in DC microgrids [18]–[30]. Voltage-based droop methods have been presented for power sharing among DC sources [19] by implementing a virtual resistor in the control system of DC sources. Droop based power and energy management strategies are given in [9], [10], [12] where the droop characteristics of batteries can be modified considering the corresponding SoC level. However, this approach cannot appropriately equalize the SoC level of distributed storages. Furthermore, one battery with higher SoC can also charge another battery with lower SoC, where the overall system efficiency decreases. A consensus protocol-based control algorithm is presented in [31] to control the power and energy management in clusters of microgrids, where the SoC information of batteries are communicated among the battery control units. Furthermore, in this approach, the control system equalizes the SoC of batteries in the clusters without taking into account charging battery storage of one microgrid by battery storage of another microgrid will decrease system efficiency and battery lifetime.

Power sharing and energy management among batteries, PVs and wind turbines are presented in [11], by employing a central supervisory control unit. The central control unit monitors the SoC level of batteries and manages the charging/discharging mode of them as well as the operation mode of PV and wind turbine, i.e., operating in or under Maximum Power Point Tracking (MPPT) mode. However, the stability and reliability of the system are questionable due to the central control approach. Furthermore, in this approach, a fully charged battery can charge a battery with a low SoC level, which may affect the lifecycle of batteries as well as the overall efficiency of the system. DC bus signaling approach is employed for power sharing in DC microgrids in [29], [30], [32], where the DC link voltage level is adjusted according to mode of operation of microgrid. Hence, the DC voltage level contains the information required for power and energy management. In [33], the SoC information is communicated among the converters through power lines by injecting a sinusoidal signal by the converters. Hence, the power and energy management can be carried out with distributed methods. However, the DC link voltage quality is poor during the signaling process. Moreover, the expandability of this method is limited due to the required currents for injecting the signals [33].

In the aforementioned works, the power sharing has properly been performed without utilizing a communication system. While the energy management strategies employ communication systems or complex control structures with some limitation such as power quality deterioration. Furthermore, DC microgrid technology is a solution for future distribution systems, where clusters of microgrids will be operated [34]. Communication-based energy management approaches, which is associated with the smart grid technologies, will introduce complexity and investment costs. It may also be exposed to cyberattacks and hence be more insecure and unstable. Therefore, using a decentralized energy management approach can be a solution for the smart operation of future clusters of microgrids. In this paper, an autonomous and decentralized power sharing and energy management approach is proposed for a PV and battery-based DC microgrid. The proposed approach is based on a coordinated droop method, which can appropriately control the power flow among the different energy units as well as manage the energy level of batteries. Furthermore, the proposed approach introduces Energy Supporting and Consumption (ESC) priority for operating the different energy sources, which can improve the overall system efficiency and reliability. Both power sharing and energy management can be achieved without utilizing any supervisory control, which can bring higher reliability and stability compared to the communication-based strategies. Thus, the main contributions of this paper include:

1- Autonomous power sharing and energy management among DC sources and the grid converter known as IC can be achieved without using communication system where the output power of sources will be defined autonomously based on the SoC level of storages, available PV power and load demand.

Pre-Print

2- The proposed strategy does not need a supervisory control and communication system, consequently it is more reliable and cost-effective compared to the state-of-the-art approaches.

3- According to the proposed control strategy and ESC, discharging of a full battery into an empty battery is avoided unlike the droop-oriented approaches [11]. Hence, the efficiency of the system can be improved.

4- The proposed approach can be employed for the operation of cluster of DC microgrids, where the clusters can independently and autonomously operate without communicating with other units. This is due to the proposed autonomous control approach and ESC strategy.

5- This approach proposes a plug-and-play capability to the units since there is no central energy management system and the units operate according to the local information.

6- The secure and reliable operation of future smart grids with clusters of microgrids can be achieved due to the eliminating the communication systems and consequently the chance of cyberattacks.

This paper is organized as follows. The objectives of power and energy management and the ESC priority are explained in Section II. Section III discusses the proposed control structure for the different converters and explains the proposed power sharing and energy management strategy. The small signal stability analysis is given in Section IV. Moreover, the effectiveness of the proposed strategy is verified by simulation and experiments reported in Section V and VI respectively. Finally, Section VII summarizes achievements.

## II. Energy Supporting and Consumption (ESC) Priority Control

The main objectives of a power sharing system are to control the output power of DC sources to prevent overstressing the units and maintain the DC link voltage within an acceptable interval. It can hierarchically be performed in three levels of primary, secondary and tertiary as shown in Fig. 1 [23]. The primary control is in charge of preventing the overstressing the units and regulating the DC link voltage at the desired value defined by secondary control. The secondary control monitors the DC link voltage and regulates it at the reference value defined by the operator (DSO) in the grid connected mode or by the standard in the islanded mode. The tertiary control is associated with the grid connection and import/export power defined by the operator. In DC grids, the grid connection can be handled by the IC, where the IC behaves as a source for DC grid. Therefore, DSO can only communicate to the IC, and IC can communicate with the internal sources to find out whether to support the microgrid or absorbs the power generated by MPPT unit.

Meanwhile, the energy storages are the main part of microgrids due to the variable power of renewable energy resources. Hence, control and monitoring the power and energy of storages are of high importance. The storages should be charged to support the microgrid with the islanded mode. Therefore, an energy management strategy is required to control the energy level of batteries, and support the microgrid demand in long term. Increasing the number of microgrids, especially in the low voltage distribution level [34] makes the energy management systems more complicated. Therefore, autonomous and decentralized operation of the microgrids can introduce a cost-effective solution for future distribution systems. In the following, the proposed decentralized energy management approach is explained.

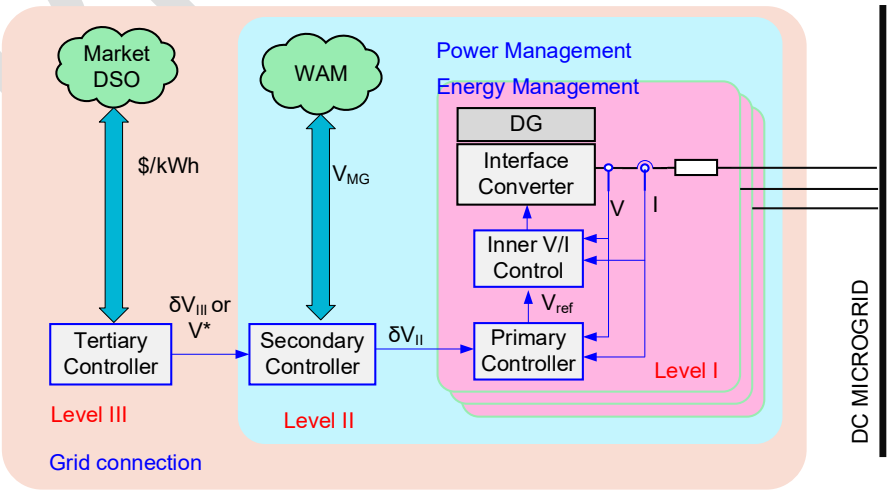


Fig. 1. Hierarchical control (three levels) structure of DC microgrids.

This paper conceptually presents a power and energy management strategy for DC microgrids. Therefore, both loads and generations should be appropriately operated in order to increase the overall efficiency and reliability of the system. Hence, an Energy Supporting and Consumption (ESC) priority is proposed to improve

the system performance. The ESC strategy is based on the priority list given in Fig. 2. For generation, the first priority is to support the microgrid demand by the PV. Hence the PV reaches the MPPT power, the IC starts to support the microgrid. If the demand of the microgrid is higher than the PV and IC, the battery will supply the loads. At the consumption side, the load has priority over other demands and it can be supported by the PV, IC, and battery in order of priority as well. Also, the battery with a low SoC level needs to be charged by the PV and IC. Finally, the extra PV power can be injected to the grid by the IC. In the case of no need for PV power, it should operate under no MPPT power. Furthermore, if the generation capacity cannot support the load, the load shedding strategy should be applied to the non-critical loads. Therefore, the ESC strategy can be summarized as follows:

- The PV has the highest generation priority to produce the maximum available power, which is also named MPPT power.
- The load has the highest consumption priority.
- If the load is supported and the battery is empty, it should be charged by the PV and IC in the order of the priority selected.
- If the PV power excess the load and battery charging power, it can be injected into the grid if it is allowed by the DSO.
- If the PV power is higher than the load, battery and IC power, the PV will operate under MPPT power.
- The upper and lower limits of the IC can be determined by the DSO or the power rating of the corresponding converter.
- If the sources cannot support the load, the non-critical loads should be disconnected (load shedding).
- In order to increase the battery lifetime, the batteries require having an SoC equalizing the control during charging and discharging.
- The batteries are only discharged in order to supply the loads. Otherwise, they should be charged or be off.

The proposed control approach explained in the next section fulfills the ESC priority in order to have a high-performance operation of the DC sources and storages.

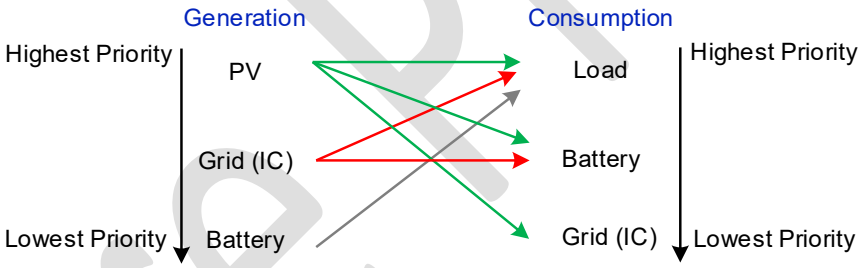


Fig. 2. Energy Supporting and Consumption (ESC) priority strategy for a DC microgrid including batteries, PV and interlinking converter to the grid.

Pre Print

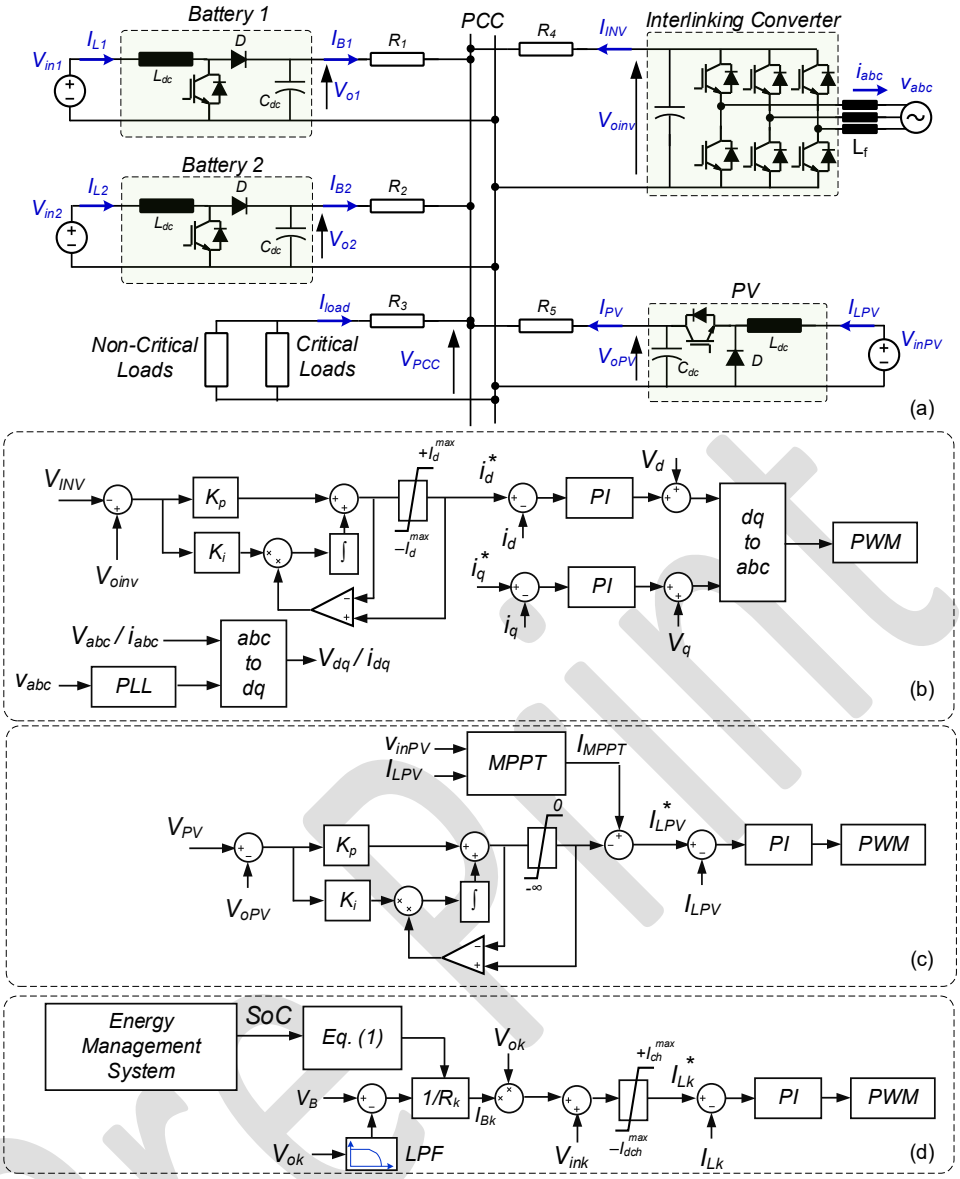


Fig. 3. Block diagram of (a) a typical dc MG, (b) IC control structure, (c) PV control structure, (d) battery control structure.

## III. Proposed Control Strategy

The DC microgrid topology and the proposed control structure are shown in Fig. 3. In order to fulfill the ESC priority, the reference voltage of the IC ($V_{INV}$) is selected higher than the reference voltage of the batteries ($V_B$). Furthermore, the PV is considered to work in MPPT whenever, the DC link voltage is lower than the maximum allowable voltage ($V_{max}$). Therefore, three operation modes can be assumed for the proposed control system as shown in Fig. 4. In Mode I, the IC regulates the DC link voltage to $V_{INV}$, as shown in Fig. 3(b), and hence, the DC voltage is formed by the IC. Since the DC voltage is lower than $V_{PV}$, as shown in Fig. 3(c), the output of the voltage regulator is saturated to zero and the PV will operate in MPPT mode. Moreover, the DC link voltage is higher than the batteries reference voltage, and hence they can be charged if required.

Therefore, in this mode, the PV operates in MPPT mode, the IC is supporting the microgrid and the batteries can be charged in the case of lower SoC level, and hence the ESC priority is carried out.

Once the MPPT current of the PV goes higher than the total currents of the load, the batteries, the IC and the DC link voltage will be increased. Therefore, the voltage regulator of the PV unit shown in Fig. 3(c) detects the overvoltage and decreases the output power in order to keep the voltage in $V_{max}$. Regulating the DC link voltage by the PV is considered as Mode III.

Preprint

Moreover, in Mode II, the PV is operating in MPPT and the IC is working in the current controlled mode, and hence the DC link voltage is formed by the batteries. Depending on the microgrid loads and SoC level of the batteries, they can be charged or discharged to manage the power and energy of the microgrid. Whenever the DC link voltage is equal or lower than $V_{min}$, the load shedding strategy should be applied to restore the microgrid voltage, and hence the non-critical loads need to be disconnected.

As can be seen from Fig. 4(a), the transition among different modes should be passed through Mode II. Therefore, a flow chart of the mode transition among the three modes and shedding can be shown as Fig. 4 (b). The equivalent circuit of the microgrid in different operating modes is also shown in Fig. 5(a-c) and it is explained in the following.

**Mode I:** In this Mode, the IC forms the DC link voltage and regulates it to $V_{INV}$. The PV operates in MPPT and can be modeled as a current source. Since the DC link voltage is higher than the reference voltage of the batteries, following Fig. 3(d), they can only be charged by a DC current of $(V_{INV} - V_B)/R_{dk}$, where $R_{dk}$ is the droop gain of the $K^{th}$ battery. $R_{dk}$ can be defined taking into consideration the SoC level of the batteries. An adaptive droop gain presented in [31] is utilized in order to equalize the SoC level of the batteries as:

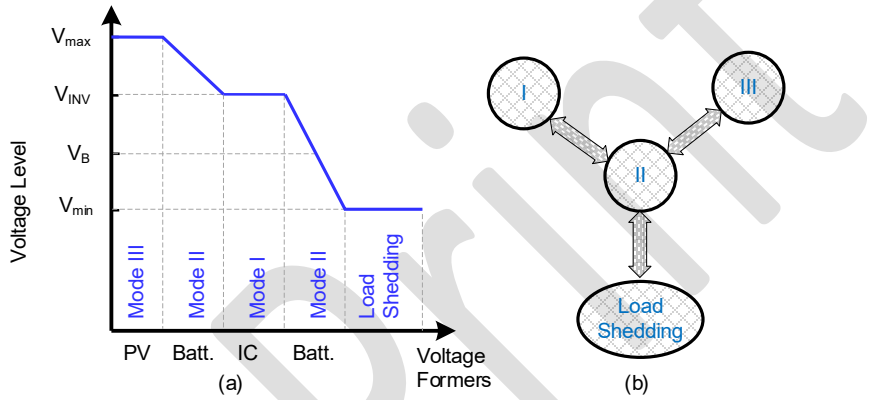


Fig. 4. Different operating modes of system, (a) voltage level in terms of voltage formers, (b) mode transition flow chart.

$$\begin{cases} R_{dk,ch} = \dfrac{C_{bk}}{C_{b\,max}}.\alpha.\left(\dfrac{1}{1-SoC_k}\right)^{\beta} \\ R_{dk,d\,ch} = \dfrac{C_{bk}}{C_{b\,max}}.\alpha.\left(\dfrac{1}{SoC_k}\right)^{\beta} \end{cases}, \qquad (1)$$

Where $C_{bk}$ is the capacity of the $K^{th}$ battery and $C_{bmax}$ is the capacity of the largest battery in the microgrid, and α and $\beta$ are positive constants determining the minimum value of droop gain and the SoC-equalizing speed. The charging and discharging droop gains in terms of SoC level are graphically shown in Fig. 6 for $C_{b2} = C_{b1} = C_{bmax}$, $\alpha = 0.1$ and $\beta = 3$. As it is shown in this figure, during charging a battery, the droop gain is increased by growing the SoC level. Following the control system of battery in Fig. 3(d), increasing the droop gain will decrease the charging current. Hence the charging current of a battery with higher SoC will be smaller than that of a battery with lower SoC level. This will equalize the SoC level of the batteries during the charging process. Furthermore, during discharging, a battery with lower SoC has a higher droop gain and hence lower discharging current, in which the SoC levels can be equalized during discharging as well.

In this mode, the DC voltage is regulated by the IC to $V_{INV}$ which is higher than $V_B$, and hence the batteries in this mode stay in charging mode. The equivalent circuit of the system can be shown like Fig. 5(a), implying that the DC voltage is controlled by the IC, and the PV and batteries are working in current controlled mode. The charging current of batteries is determined by the droop gains ($R_{dk}$), where in the lower SoC, the batteries will be charged by the maximum rated current of the battery converter as shown in Fig. 3(d). To check the ESC priority, it is fruitful to mention that:

1) The PV is always operating at MPPT mode.
2) The load is connected to the DC bus and will always be supported by the microgrid.
3) The batteries are in charging mode and will not be discharged into the grid or load.
4) The battery with the lowest SoC will be charged faster than the one with higher SoC.
5) Since the IC is regulating the DC voltage at $V_{INV}$, it balances the current among the PV, load, batteries and the grid.

Pre-Print

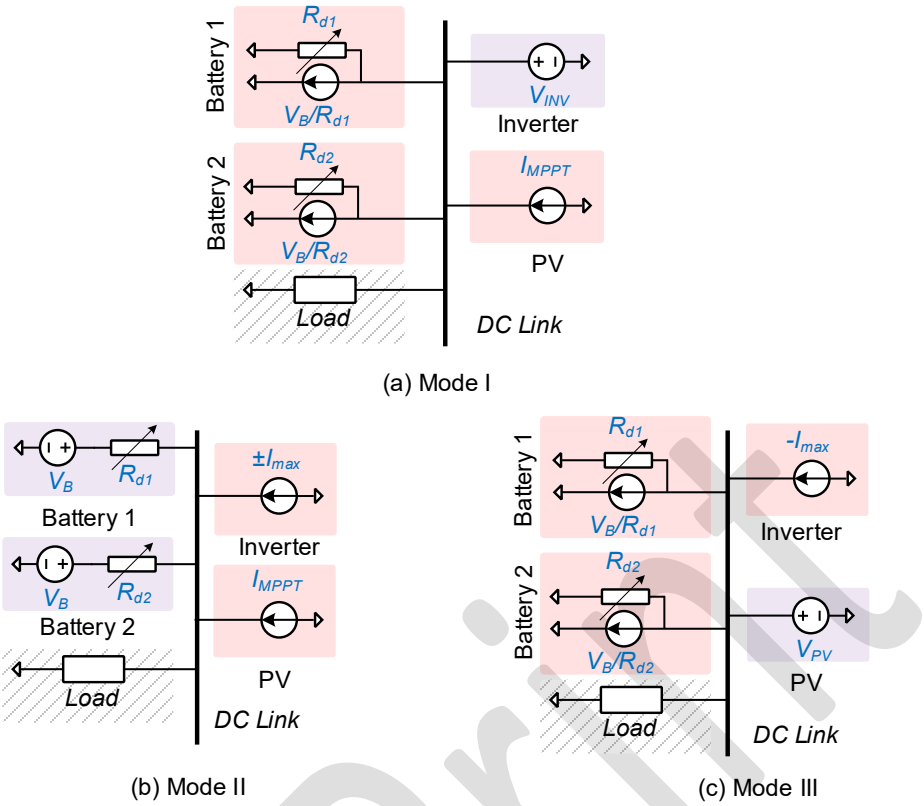


Fig. 5. Equivalent circuits of the system under different operation modes; (a) Mode I: inverter control mode, (b) Mode II: battery control mode, (c) Mode III: PV control mode.

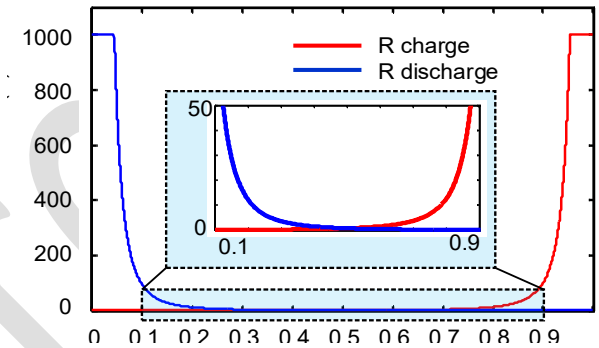


Fig. 6. Adaptive droop gains for charging and discharging states in terms of SoC level of batteries.

**Mode II:** Once the IC reaches the maximum current ($\pm I_{max}$), it operates in current control mode as shown in Fig. 3(b). Therefore, the batteries are operating in droop mode to control the DC link voltage. The equivalent circuit of the system in Mode II is shown in Fig. 5(b).

According to the control system of the IC shown in Fig. 3(b), if the DC link voltage is higher than $V_{INV}$, the IC needs to absorb the maximum current from the DC microgrid. Furthermore, the batteries are in charging mode as shown in Fig. 5(b), since the DC voltage is higher than $V_B$. Therefore, the batteries will not be discharged to the grid in this mode. The PV is working at MPPT and the batteries are charging taking into account the corresponding SoC level. Moreover, if the DC voltage is lower than $V_{INV}$, the IC injects the maximum current into the DC microgrid. Now, if the DC voltage is higher than $V_B$, the batteries are in charging mode. Furthermore, the PV is operating in MPPT mode. Once the DC voltage goes lower than $V_B$, which means none of the PV and IC can supply the loads, the batteries need to discharge to support the load. Hence the ESC priority is also fulfilled in this mode, where at first the PV operates in MPPT mode, and then the IC injects the maximum current and finally, the batteries supply the remaining load. In this mode, the charging and discharging of batteries are equalized by the SoC-equalizing droop gains.

**Mode III:** Moreover, in the case that the PV power is higher than the charging current of the batteries, load, and the IC power, the DC link voltage will increase. In this condition, the PV needs to reduce the MPPT power

to keep the voltage at $V_{PV}$. In this mode, the ESC priority can also be fulfilled since the load is supported, the batteries are in charging mode and the remaining current of the PV can be injected into the grid. The equivalent circuit of this Mode can be illustrated as shown in Fig. 5(c).

## IV. Small Signal Stability Analysis

In order to design the power loop control parameters and ensuring a stable operation in different operation modes, small signal stability analysis is provided in this section. Following Fig. 3(a), for the DC bus the KCL yields:

$$I_{INV} + I_{PV} + I_{B1} + I_{B2} + I_{Load} = 0 \tag{2}$$

Furthermore, according to Fig. 3(d), considering the inner current loop to be fast enough and the feeder impedances to be negligible, the battery current can be found as follows:

$$I_{Bk} = \frac{V_B - G_{LPF}(s)V_d}{R_{dk}}, \tag{3}$$

where, $V_d$ is the DC link voltage and

$$G_{LPF}(\mathrm{s}) = \frac{1}{1+sT}, \tag{4}$$

is a low pass filter with a time constant of $T$. The load current in Fig. 3(a), $I_{Load}$, can also be expressed as follows:

$$I_{Load} = -P_{Load} \big/ V_d \tag{5}$$

where, $P_{Load}$ is the load power. The load is modeled as a constant power load. The KCL in (2) can be rearranged as follows.

$$I_{INV} + I_{PV} = \frac{G_{LPF}(s)V_d - V_B}{R_{d1}} + \frac{G_{LPF}(s)V_d - V_B}{R_{d2}} + \frac{P_{Load}}{V_d} \tag{6}$$

According to Fig. 3(a, b) and the electrical model represented in Fig. 5, the IC current can be written as follows:

$$I_{INV} = \begin{cases} G_{V,INV}(\mathrm{s}) \cdot (V_{INV} - V_d) & Mode\ I \\ \pm \mathrm{I}_{max} & Mode\ II \\ -\mathrm{I}_{max} & Mode\ III \end{cases} \tag{7}$$

and PV current can be obtained as follows:

$$I_{PV} = \begin{cases} I_{MPPT} & Mode\ I \\ I_{MPPT} & Mode\ II \\ G_{V,\mathrm{PV}}(\mathrm{s}) \cdot (V_{PV} - V_d) & Mode\ III \end{cases} \tag{8}$$

where, $G_{V,INV}$ and $G_{V,PV}$ are the Proportional-Integrator (PI) regulators for voltage loop. The linear form of the KCL equation in (6) can be written as:

$$\Delta I_{INV} + \Delta I_{PV} = \frac{G_{LPF}(s)\Delta V_d}{R_{d1}} + \frac{G_{LPF}(s)\Delta V_d}{R_{d2}} - \frac{P_{Load}}{V_{d0}^2}\Delta V_d \,. \tag{9}$$

The linear form of the IC and PV currents can be found as (10) and (11) respectively.

$$\Delta I_{INV} = \begin{cases} -G_{V,INV}(\mathrm{s}) \cdot (\Delta V_d) & Mode\ I \\ 0 & Mode\ II \\ 0 & Mode\ III \end{cases} \tag{10}$$

$$\Delta I_{PV} = \begin{cases} 0 & Mode\ I \\ 0 & Mode\ II \\ -G_{V,\mathrm{PV}}(\mathrm{s}) \cdot (\Delta V_d) & Mode\ III \end{cases} \tag{11}$$

Considering

$$G_v(s) = \begin{cases} G_{V,\mathrm{INV}}(\mathrm{s}) & Mode\ I \\ 0 & Mode\ II \\ G_{V,\mathrm{PV}}(\mathrm{s}) & Mode\ III \end{cases}, \tag{12}$$

Pre Print

the linear form equation (9) can be rearranged as follows:

$$\left( G_v(s) + \frac{G_{LPF}(s)}{R_{d1}} + \frac{G_{LPF}(s)}{R_{d2}} - \frac{P_{Load}}{V_{d0}^2} \right) \Delta V_d = 0 . \quad (13)$$

Putting the controller transfer function as:

$$G_v(s) = K_p + {K_i}/{s} , \quad (14)$$

the characteristic equation of the closed loop system of dominant poles relevant to the power sharing control, can be represented as follows:

$$\begin{aligned} & a_2 \cdot s^2 + a_1 \cdot s + a_0 = 0; \\ & a_2 = \left( K_p - \frac{P_{Load}}{V_{d0}^2} \right) T, \\ & a_1 = \frac{1}{R_{d1}} + \frac{1}{R_{d2}} + \left( K_p - \frac{P_{Load}}{V_{d0}^2} \right) + K_i T, \\ & a_0 = K_i . \end{aligned} \quad (15)$$

According to the Routh-Hurwitz stability criterion, the system is stable if, and only if, the coefficients of $a_0$, $a_1$ and $a_2$ in (15) have positive values. Therefore, to maintain the system stability, the voltage regulator proportional gain, $K_p$, must be greater than $P_{Load}/V_{d0}^2$. In this condition, the coefficients $a_0$, $a_1$ and $a_2$ will be positive, consequently, the overall system will be stable.

## V. Simulation Results

In order to evaluate the proposed power sharing and energy management approach, two simulation case studies are considered and the simulation results are explained in the following. The system and control parameters are given in Table I. Since the maximum generation capacity is 30 *A* which is equal to 12 *kW*, according to (15), the system stability is guaranteed since the voltage regulators proportional gain $K_p$ = 0.2 is greater than $P_{Load}/V_{d0}^2 = 12{,}000/400^2 = 0.075$. As $K_p > P_{Load}/V_{d0}^2$ for the maximum load of system, i.e., 12 *kW*, it will be stable for other loading conditions as well. The simulation results reported in the following illustrate the stability of the system at different operating conditions where the overall system stability is achieved under the designed control parameters given in Table I.

In the following, three case studies are considered in order to examine the effectiveness of the proposed control strategy at different loading and generation conditions. The simulation results are demonstrated in Fig. 7, Fig. 8 and Fig. 9, and the microgrid operation mode at each time is mentioned at the top of the corresponding figures.

**Case I:** In this case, the batteries, PV, and IC are connected to the grid. The initial SoC level of battery B1 and B2 are considered to be 80% and 20% respectively. Furthermore, the IC is not allowed by the DSO to inject power into the grid, and hence, the its power is limited to solely support the microgrid and its DC current should be between 0 and $I_{max}$. Notably, according to Fig. 3(a), $0 < I_{INV} < I_{max}$. Simulation results including output current of the converters, DC link voltage and SoC level of batteries in terms of load variation are shown in Fig. 7. The transient events are explained in the following.

TABLE I: Parameters of the microgrid and the control system

| Definition | Symbol | Simulation | Test |
|---|---|---|---|
| Boost Converter for Battery | Rated current *(A)* | 5 | 0.8 |
| | voltage regulator | 0.2 + 5/s | 0.2 + 5/s |
| | Inner current regulator | 0.05 + 1/s | 0.05 + 1/s |
| | $L_{dc}$ *(mH)*, $C_{dc}$ *(μF)* | 2, 560 | 2, 560 |
| Boost Converter for PV | Rated Current *(A)* | 10 | 1.4 |
| | voltage regulator | 0.2 + 5/s | 0.2 + 5/s |
| | Inner current regulator | 0.05 + 1/s | 0.05 + 1/s |
| | Frequency regulator | 0.35+2/s | 0.35+2/s |
| | $L_{dc}$ *(mH)*, $C_{dc}$ *(μF)* | 2, 560 | 2, 560 |
| Inverter | Rated current *(A)* | 10 | 1.2 |
| | voltage regulator | 0.2 + 5/s | 0.2 + 5/s |
| | Inner current regulator | 0.02 + 2/s | 0.02 + 2/s |
| | $C_{dc}$ *(μF)* | 560 | 560 |
| | *Power Factor*($i_a^*$) | 1 (0) | 1 (0) |
| | $L_f$ *(μH)*, $C_f$ *(μF)* | 1.2, 20 | 1.2, 20 |
| DC Voltage Levels | $V_{max}$ *(V)* | 410 | 102 |
| | $V_B$ *(V)* | 400 | 99 |

Pre Print

| | | | |
|---|---|---|---|
| | $V_{INV}$ (V) | 405 | 100 |
| | $V_{min}$ (V) | 380 | 98 |
| AC grid | $V_{abc}$ ($V_{peak}$), $f$ (Hz) | 180, 50 | 60,50 |

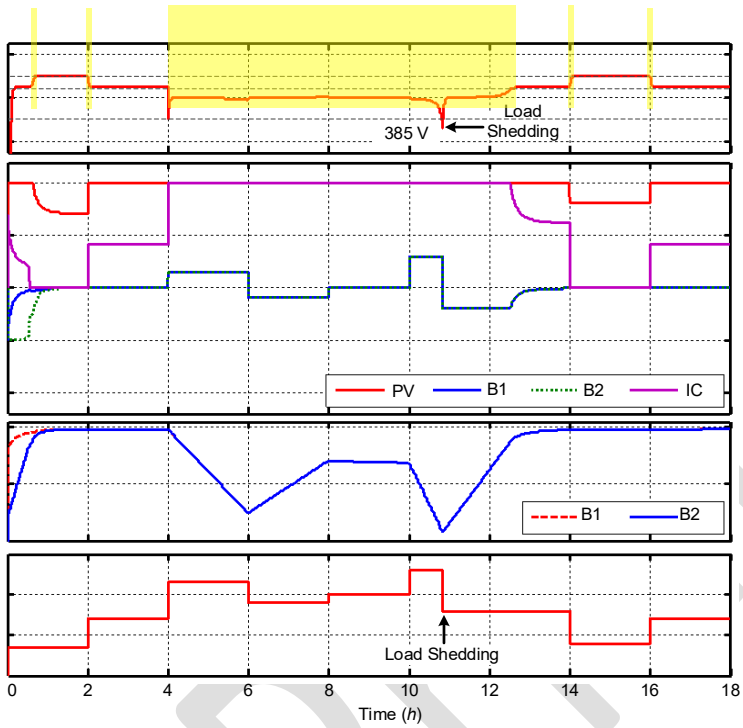


Fig. 7. Simulation results of power sharing and energy management in the microgrid following the load variation in Case I.

During $0 < t < 0.6$ $h$, the total load demand is 7 $A$ and the MPPT current of the PV is 10 $A$. Since the batteries are not fully charged, the extra current of the PV needs to charge them. However, the required charging currents of batteries are higher than the excess current of PV, and hence the IC needs to support the batteries. In this condition, the IC controls the DC link voltage at 405 $V$. Moreover, the SoC level of battery B2 is lower than battery B1, and hence the charging current and charging rate of battery B2 is higher than battery B1 in order to equalize the corresponding SoC levels.

During $0.6 < t < 2$ $h$, the SoC level of batteries is equalized and the batteries are fully charged. Therefore, the load must be supplied by the PV and IC. Since, the PV has the highest priority according to Fig. 2, it should supply the load at first. If the load power is higher than the PV MPPT power, the remaining load should be supplied by the IC. However, in this case, the PV MPPT power is higher than the load power. Therefore, the load is totally supported by the PV. Since the generation is higher than the load, the DC link voltage will go up as it can be seen from Fig. 7 at $t > 0.6$ $h$. Following Fig. 3(b), the output of the IS's voltage controller will be saturated at the lowest limit of the current. Since the IC is not allowed to inject the power into the grid by DSO, the lower limit is set to zero and the output current of IC will be zero as shown in Fig. 7. Therefore, the PV control system makes it to operate under MPPT mode. In this condition, the PV regulates the DC link voltage at 410 V.

During $2 < t < 4$ $h$, the load increases to 14 $A$ and with following the priority, PV and IC supply 10 and 4 $A$ respectively. Hence the PV is operating in MPPT mode, and the IC controls the DC link voltage at 405 $V$.

During $4 < t < 6$ $h$, the load increases to 22 $A$. The maximum currents of PV and IC are higher than the load demand, and then the batteries supply the remaining current of the load. As it can be seen, the battery currents are equal and the corresponding SoC variations are the same during discharging. In this period, the voltage of the DC link is controlled by batteries working in droop mode.

During $6 < t < 8$ $h$, the load is decreased by 4 $A$. Since the SoC levels of batteries are low, the IC and PV supply the maximum current to support the load as well as charge the batteries. Therefore, the batteries are working in droop mode and controlling the DC link voltage. Furthermore, the charging rate and current of batteries are equal. When the load is equal to 20 $A$ during $8 < t < 10$ $h$, the IC and PV can only support the load, and hence the batteries cannot be charged. However, since the PV and IC are working at maximum current, the DC link voltage is controlled by batteries.

Increasing the load to 26 *A* at *t* = 10 *h*, the batteries are starting to support the load together with the IC and PV. Once the batteries are discharged, the load cannot be supported, and the DC link voltage is decreasing. Therefore, when the DC link voltage is equal to 385 *V*, a non-critical load is shed. After load shedding at *t* = 10.6 *h*, the batteries are charging with a maximum charging current. Once they are charged, the IC current decreases at *t* = 12.5 *h* and the load is supplied by the PV and IC. The operating condition during 14 *h* to 18 *h* is similar to the operating condition from 1 to 4 *h*.

**Case II**: In this Case, the performance of the proposed energy management strategy is further demonstrated and the simulation results are shown in Fig. 8. The initial SoC levels of batteries B1 and B2 are equal to 0 and 50% respectively. Therefore, the batteries are charged by the PV and IC. Since the SoC of battery B1 is lower than battery B2, the charging current of B1 is higher than battery B2. Therefore, the charging rate of battery B1 is higher than battery B2 in order to equalize the corresponding SoC levels. Once the SoC of battery B2 is close to 100%, it's charging current is decreased, and hence the IC current is decreased. When the battery B2 is fully charged, the IC current is further decreased. After charging the batteries, the PV and IC supply the load.

At *t* = 4 *h*, the battery B2 is disconnected and the load current is equal to 22 *A*. Therefore, the PV, IC, and battery B1 supply the load. Following the priority, the PV and IC are operating at maximum current, and the remaining load is supported by the battery. At *t* = 5 *h*, the battery B2 is reconnected. Since the SoC level of battery B2 is higher than battery B1, the output current and discharging rate of battery B2 are higher than battery B1 in order to equalize the corresponding SoC levels.

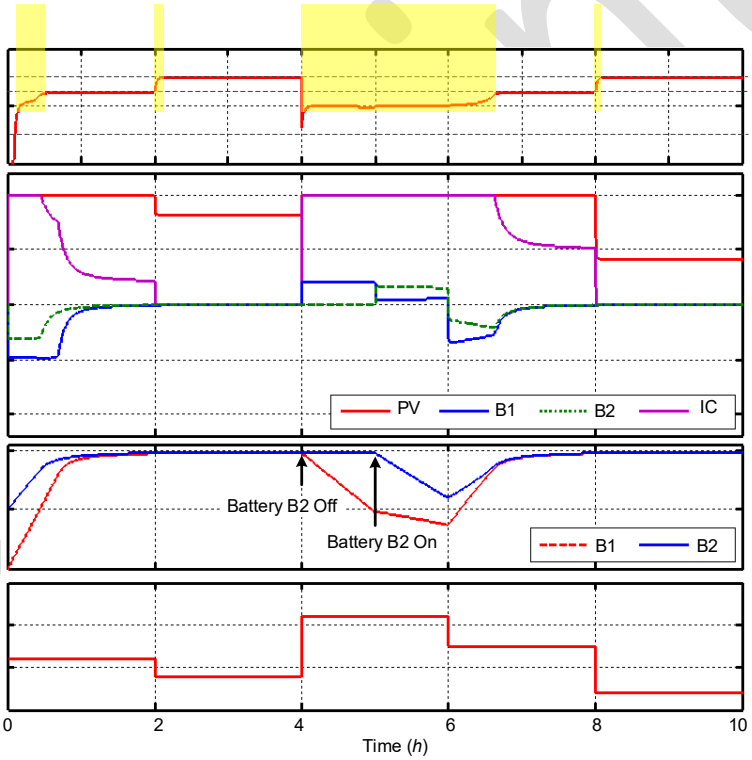


Fig. 8. Simulation results of power sharing and energy management in the microgrid following the load variation in Case II.

At *t* = 6 *h*, the load is decreased by 6 *A*. Therefore, the PV and IC can recharge the batteries. Since at this time, the SoC of battery B1 is lower than battery B2, the charging current and rate of battery B1 is higher than battery B2. Once both batteries are fully charged, the IC decreases its current and the PV operates in MPP.

Moreover, at *t* = 8 *h*, the load is decreased to 4 *A*. Following the ESC priority, the load should be supplied by the PV. Hence the PV operates under MPPT mode to support the load as well as to control the DC link voltage.

**Case III:** In this Case, the IC is allowed by the DSO to inject the current into the grid up to 5 A. Furthermore, the control system performance in the absence of the grid and/or PV is demonstrated.

During 0 < *t* < 2 hour, the battery B2 is disconnected, battery B1 is fully charged, and the load is 14 A. Hence, according to the priority list, the PV is supplying 10 A in MPPT mode and the IC is supporting 4 A, and the output current of battery B1 is equal to 0 A. At *t* = 2 *h*, the battery B2 is reconnected and the load is decreased to 4 A. Based on the priority list of consumption, at first the load is supported, then battery B2 is charged with the maximum current. The excess current of the PV equals to 1 A is injected to the grid by the IC. Once the battery is charged at *t* = 2.8 *h*, the PV current is injected into the grid. Since the load current equals to 4 A, and the

maximum current of the IC is limited to 5 A, the PV is operated under MPPT mode in order to balance the generation and demand.

During $4 < t < 6$ $h$, the load is 8 A and hence the PV is supporting the load. Since the batteries are fully charged, the excess power of the PV is injected into the grid through the IC.

During $6 < t < 7$ $h$, the load is 22 A, and following the priority, the load is supported by the PV and IC. However, the maximum current supplied by the PV and IC is 20 A. Hence the remaining load is supplied by the batteries. Since the batteries have the same SoC levels, the load is equally shared between them. At $t = 7$ $h$, the load is decreased to 16 A, and the PV is operating at MPPT. Since the IC can support up to 10 A, at first, the batteries are charged. After charging them, the IC decreases the output current.

During $8 < t < 11$ $h$, the PV is turned off, the IC is operating at maximum current mode and the demand and generation are balanced by the batteries.

During $11 < t < 12$ $h$, the IC is turned off, and the PV is reconnected to the grid. At first, the PV supports the load and charges the batteries. Once the batteries are charged, the PV operates under MPPT power. Moreover, at $t = 12$ $h$, the PV is also disconnected, and the load is supported by the batteries. The batteries are equally discharged. When the energy of batteries is discharged, the voltage will drop below 385 V, hence, the loads will be disconnected.

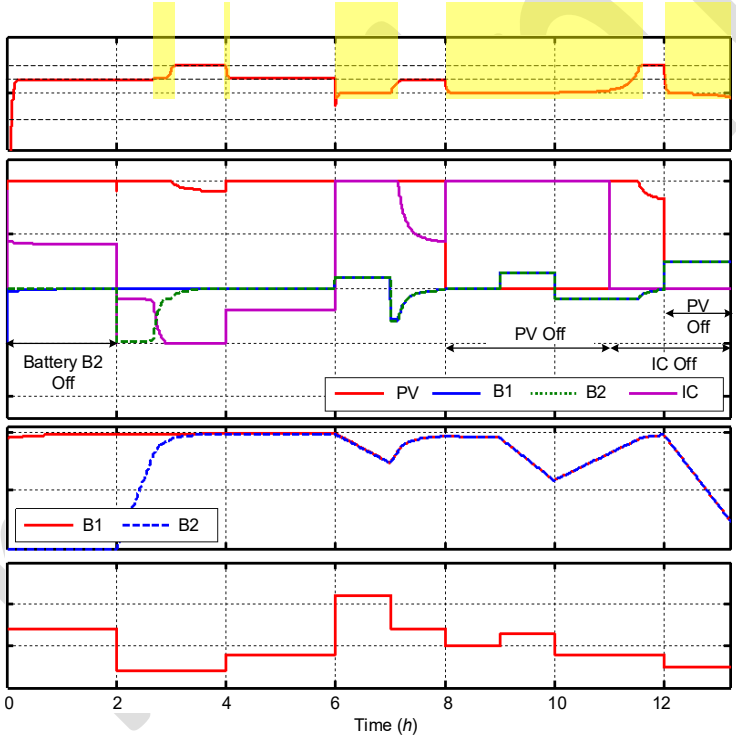


Fig. 9. Simulation results of power sharing and energy management in the microgrid following the load variation in Case III.

## VI. Experimental Results

In order to further validate the performance of the proposed control approach, some experiments have been performed in a laboratory prototype. A photograph of the implemented test setup is shown in Fig. 10 which includes two bidirectional DC/DC boost converters and a three-phase inverter. One Digital Signal Processor (DSP) is used to control the two DC converters and another DSP is used to control the inverter. The parameters of the implemented test setup and the control system are given in TABLE I. The experimental results are reported in the following.

In the first test, a 170 $W$ load is supported by the IC and battery B1. The battery B2 is disconnected. Therefore, as shown in Fig. 11, the IC is supporting the rated current of 1.2 $A$, and the battery B1 is supplying 0.5 $A$. Since the IC is working at rated current, the DC voltage is controlled by B1 and it is equal to 99 $V$. Hence the system is operating in Mode II. Once the load is decreased to 60 $W$, the output currents of IC and B1 are decreased and the DC link voltage is regulated at 100 $V$ by the IC. Therefore, the system is working in Mode I. Following the ESC priority, in Mode II, the IC supporting the maximum current and the remaining load is supported by the battery. Once the load is decreased, the output current of the battery is equal to zero and the load is supplied by the IC.

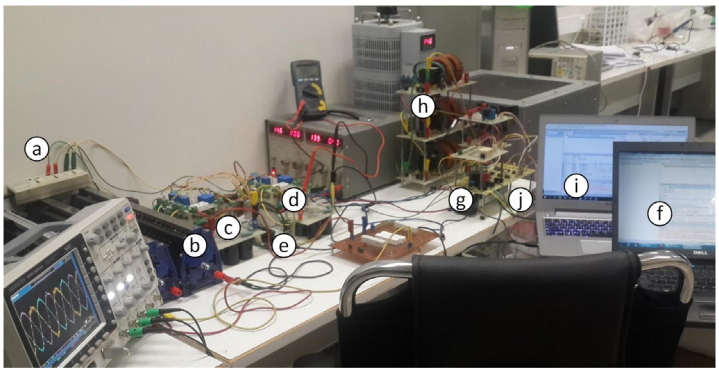


Fig. 10. Photograph of the implemented hardware setup: (a) input DC power for DC/DC converters, (b) DC load, (c, d) DC/DC boost converters, (e) DSP of boost converters, (f) control center of boost converters, (g) three phase inverter (IC), (h) filter of inverter, (i) control center of inverter, and (j) DSP of inverter.

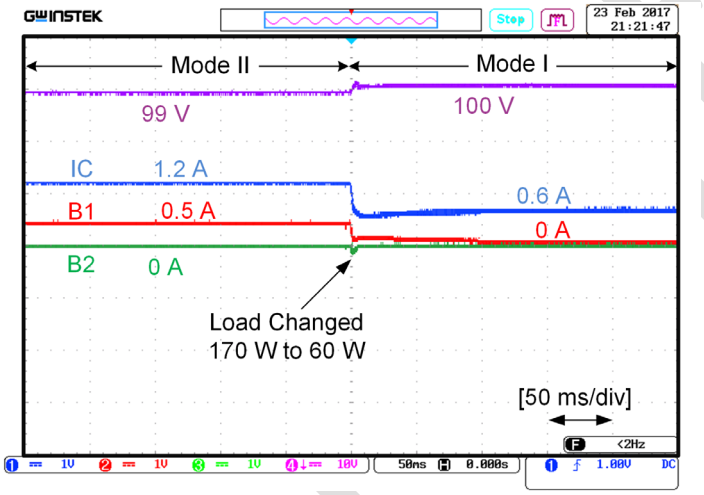


Fig. 11. Experimental results: Operating in Mode I and Mode II with a battery (B1) and an IC.

In the next test, the second battery B2 with a lower SoC is connected to the grid. As shown in Fig. 12, at first, the load is supported by the battery B1 and the IC, and the IC is operating at rated current. Hence, the voltage is controlled by B1 and it is equal to 99 *V*. Once the load is reduced by 100 *W*, according to the ESC priority, the output current of B1 is settled at zero, and the second battery is started to be charged. Based on the proposed ESC priority, battery B2 with a lower SoC is charging and the battery B1 cannot be discharged to B2. Moreover, since B2 is empty, the IC needs to be operated at rated current to charge it. In this test, the DC link voltage is controlled by the batteries and the system is in Mode II.

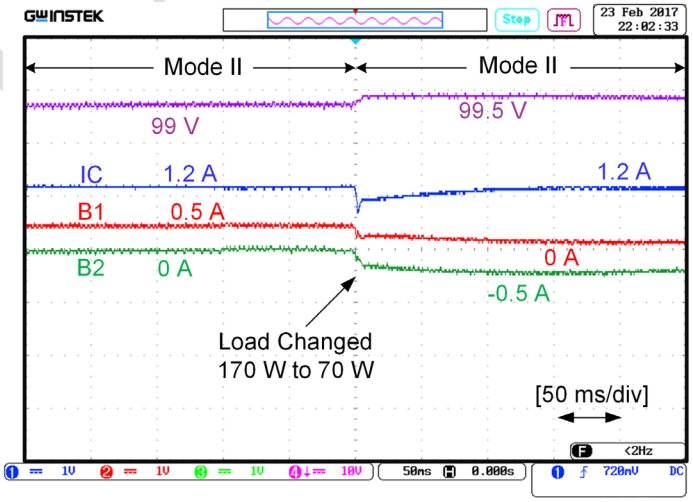


Fig. 12. Experimental results: Operating in Mode II with an IC and two batteries (B1, B2) with SoC B1 = 100% and SoC B2 = 0%.

In order to evaluate the performance of the control system in the presence of MPPT based sources, a PV, battery and an IC are considered and the current sharing result is shown in Fig. 13. The PV is working in MPPT mode with 1.4 *A* output current. The SoC of the battery is low and the dc load is 160 *W*. Hence, the output current of IC is 1 *A* supporting the load and charging the battery. Once the load is decreased by 40 *W*, according to the ESC priority, the PV is working in MPPT mode, the battery is charging and the output current of IC is decreased. The voltage is regulated by the IC at 100 *V*, and thus the system is working in Mode I.

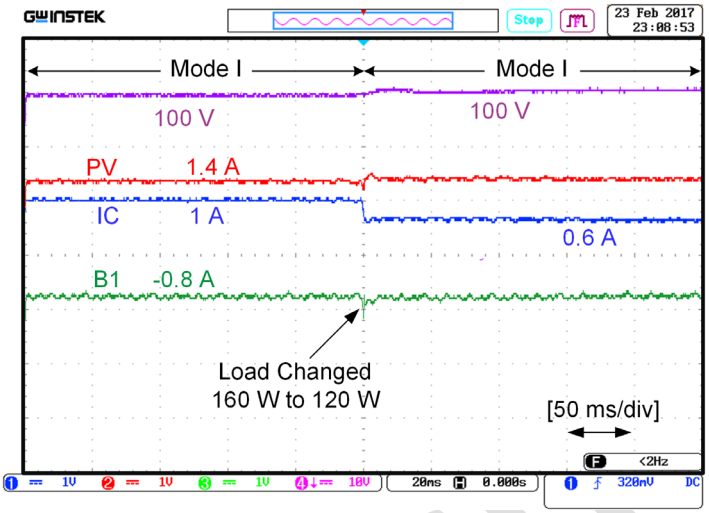


Fig. 13. Experimental results: Operating in Mode I with a battery (B1), a PV and an IC.

In the next test, the PV is operating in MPPT mode with an output current of 1.1 *A* as shown in Fig. 14. The PV and IC supporting a 70 *W* load and the battery. The DC link voltage is controlled by the IC to be 100 *V*, and the system is operating in Mode I. When the battery is fully charged, the only demand from the microgrid is the 70 *W* load. Following the ESC priority, the IC has to reduce the output current. Furthermore, it is considered that the IC is not allowed to inject the current to the grid. Therefore, the PV needs to work under MPPT mode, and hence, the DC link voltage is controlled by the PV to be regulated to 102 *V* and the system is working in Mode III.

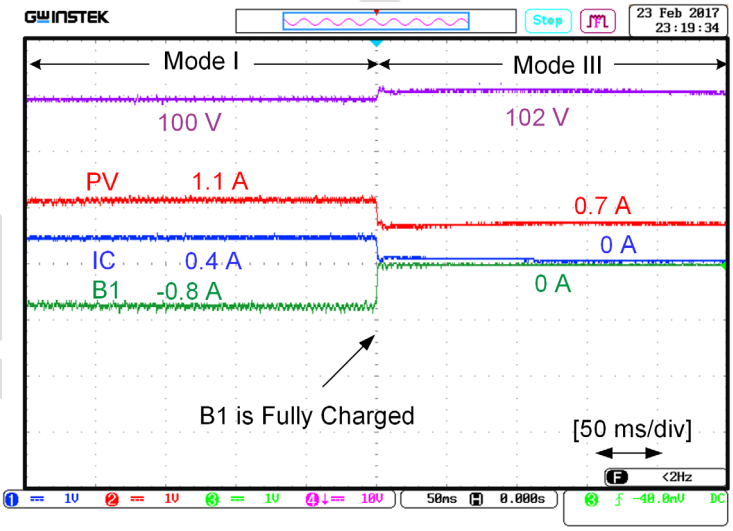


Fig. 14. Experimental results: Operating in Mode I and Mode III with a battery (B1), a PV and an IC.

## VII. Conclusion

This paper proposes an autonomous power sharing and energy management strategy for DC microgrids. The proposed approach does not require supervisory control and communication infrastructure. Thereby, it introduces a reliable operation and a cost-effective solution for DC microgrids in power sharing and energy management level. The operation of PV unit and IC can appropriately be managed based on the proposed ESC strategy employing the local voltage information. Moreover, following the proposed control strategy, the SoC level of batteries can properly be equalized and the power flow from a full battery to an empty battery is avoided. Consequently, the life-cycle of the batteries and the overall system efficiency can be enhanced. Moreover, this approach introduces a plug and play capability to the microgrid, where each battery unit can properly operate

based on its individual control system and local voltage information without communicating a central energy management unit. The effectiveness of the proposed strategy is evaluated under different simulation case studies and validated by experiments. The obtained results show that the different energy sources can properly support the microgrid following the load power and SoC level of batteries. As a future research, the proposed control strategy can be modified for the use of different MPPT based units. Furthermore, the autonomous operation of clusters of DC microgrids without communication systems will be explored in the future.

## References


[1] S. Peyghami, P. Davari, H. Mokhtari, and F. Blaabjerg, "Decentralized Droop Control in DC Microgrids Based on a Frequency Injection Approach," *IEEE Trans. Smart Grid*, vol. 99, no. To be published/DOI: 10.1109/TSG.2019.2911213, pp. 1–11, 2019.

[2] S. P. Barave and B. H. Chowdhury, "Hybrid AC/DC Power Distribution Solution for Future Space Applications," in *Proc. IEEE Power Engineering Society General Meeting*, 2007, pp. 1–7.

[3] H. Zhang, F. Mollet, C. Saudemont, and B. Robyns, "Experimental Validation of Energy Storage System Management Strategies for a Local DC Distribution System of More Electric Aircraft," *IEEE Trans. Ind. Electron.*, vol. 57, no. 12, pp. 3905–3916, Dec. 2010.

[4] J. G. Ciezki and R. W. Ashton, "Selection and Stability Issues Associated with a Navy Shipboard DC Zonal Electric Distribution System," *IEEE Trans. Power Deliv.*, vol. 15, no. 2, pp. 665–669, Apr. 2000.

[5] B. Zahedi and L. E. Norum, "Modelling and Simulation of Hybrid Electric Ships with DC Distribution Systems," *2013 15th Eur. Conf. Power Electron. Appl.*, vol. 28, no. 10, pp. 1–10, 2013.

[6] N. Hatziargyriou, H. Asano, R. Iravani, and C. Marnay, "Microgrids," *IEEE Power and Energy Magazine*, vol. 5, no. 4, pp. 78–94, 2007.

[7] F. Katiraei, R. Iravani, N. Hatziargyriou, and A. Dimeas, "Microgrids Management," *IEEE Power Energy Mag.*, vol. 6, no. 3, pp. 54–65, 2008.

[8] N. Eghtedarpour and E. Farjah, "Distributed Charge/Discharge Control of Energy Storages in a Renewable-Energy-Based DC Micro-Grid," *Renew. Power Gener. IET*, vol. 8, no. 1, pp. 45–57, 2014.

[9] P. C. Loh, Y. K. Chia, D. Li, and F. Blaabjerg, "Autonomous Operation of Distributed Storages in Microgrids," *IET Power Electron.*, vol. 7, no. 1, pp. 23–30, 2014.

[10] P. C. Loh and F. Blaabjerg, "Autonomous Control of Distributed Storages in Microgrids," in *Proc. IEEE ECCE Asia*, 2011, pp. 536–542.

[11] T. Dragicevic, J. M. Guerrero, J. C. Vasquez, and D. Skrlec, "Supervisory Control of an Adaptive-Droop Regulated DC Microgrid with Battery Management Capability," *IEEE Trans. Power Electron.*, vol. 29, no. 2, pp. 695–706, 2014.

[12] Y. Gu, X. Xiang, W. Li, and X. He, "Mode-Adaptive Decentralized Control for Renewable DC Microgrid With Enhanced Reliability and Flexibility," *IEEE Trans. Power Electron.*, vol. 29, no. 9, pp. 5072–5080, 2014.

[13] P. C. Loh, D. Li, Y. K. Chai, and F. Blaabjerg, "Autonomous Control of Interlinking Converter with Energy Storage in Hybrid AC-DC Microgrid," *IEEE Trans. Ind. Appl.*, vol. 49, no. 3, pp. 1374–1382, 2013.

[14] S. Peyghami-Akhuleh, H. Mokhtari, P. Davari, P. C. Loh, and F. Blaabjerg, "Smart Power Management of DC Microgrids in Future Milligrids," in *Proc. IEEE EPE*, 2016, pp. 1–10.

[15] I. U. Nutkani, P. C. Loh, P. Wang, T. K. Jet, and F. Blaabjerg, "Intertied Ac–Ac Microgrids with Autonomous Power Import and Export," *Int. J. Electr. Power Energy Syst.*, vol. 65, pp. 385–393, 2015.

[16] I. U. Nutkani, P. C. Loh, and F. Blaabjerg, "Distributed Operation of Interlinked Ac Microgrids with Dynamic Active and Reactive Power Tuning," *IEEE Trans. Ind. Appl.*, vol. 49, no. 5, pp. 2188–2196, 2013.

[17] P. C. Loh, D. Li, Y. K. Chai, and F. Blaabjerg, "Autonomous Operation of Hybrid Microgrid with AC and DC Subgrids," *IEEE Trans. Power Electron.*, vol. 28, no. 5, pp. 2214–2223, 2013.

[18] N. R. Chaudhuri, B. Chaudhuri, R. Mujumder, and A. Yazdani, "*Multi-Termibal Direct-Current Grids: Modeling, Analysis and Control.*" Hoboken, New Jersey: John Wiley & Sons, 2014.

[19] J. M. Guerrero, J. C. Vasquez, J. Matas, L. G. De Vicuña, and M. Castilla, "Hierarchical Control of Droop-Controlled AC and DC Microgrids - A General Approach toward Standardization," *IEEE Trans. Ind. Electron.*, vol. 58, no. 1, pp. 158–172, 2011.

[20] A. Accetta and M. Pucci, "Energy Management System in DC Micro-Grids of Smart Ships: Main Gen-Set Fuel Consumption Minimization and Fault Compensation," *IEEE Trans. Ind. Appl.*, vol. 55, no. 3, pp. 3097–3113, May 2019.

[21] U. Manandhar, A. Ukil, H. Beng Gooi, N. R. Tummuru, and S. K. Kollimalla, "A Low Complexity Control and Energy Management for DC-Coupled Hybrid Microgrid with Hybrid Energy Storage System," in *2017 IEEE Power & Energy Society General Meeting*, 2017, pp. 1–5.

[22] M. J. Rana and M. A. Abido, "Energy Management in DC Microgrid with Energy Storage and Model Predictive Controlled AC–DC Converter," *IET Gener. Transm. Distrib.*, vol. 11, no. 15, pp. 3694–3702, Oct. 2017.

[23] S. Peyghami, H. Mokhtari, and F. Blaabjerg, "Hierarchical Power Sharing Control in DC Microgrids," in *Microgrid*, First., Magdi S Mahmoud, Ed. Elsevier Science & Technology, 2017, pp. 63–100.

[24] V. Nasirian, A. Davoudi, F. L. Lewis, and J. M. Guerrero, "Distributed Adaptive Droop Control for Dc Distribution Systems," *IEEE Trans. Energy Convers.*, vol. 29, no. 4, pp. 944–956, 2014.

[25] T. Morstyn, B. Hredzak, G. D. Demetriades, and V. G. Agelidis, "Unified Distributed Control for DC Microgrid Operating Modes," *IEEE Trans. Power Syst.*, vol. 31, no. 1, pp. 802–812, Jan. 2016.

[26] T. Morstyn, B. Hredzak, and V. G. Agelidis, "Cooperative Multi-Agent Control of Heterogeneous Storage Devices Distributed in a DC Microgrid," *IEEE Trans. Power Syst.*, vol. 31, no. 4, pp. 2974–2986, Jul. 2016.

[27] D. J. D. Perreault, R. R. L. Selders, and J. J. G. Kassakian, "Frequency-Based Current-Sharing Techniques for Paralleled Power Converters," *IEEE Trans. Power Electron.*, vol. 13, no. 4, pp. 626–634, Jul. 1998.

[28] S. Peyghami, P. Davari, H. Mokhtari, P. C. Loh, B. Frede, and F. Blaabjerg, "Synchronverter-Enabled Power Sharing Approach for LVDC Microgrids," *IEEE Trans. Power Electron.*, vol. 32, no. 10, pp. 8089–8099, Oct. 2017.

[29] X. Li, B. Liu, F. Zhuo, and G. Ning, "A Novel Control Strategy Based on DC Bus Signaling for DC Micro-Grid with Photovoltaic and Battery Energy Storage," in *Proc. China International Conference on Electricity Distribution (CICED)*, 2016, pp. 1–5.

[30] F. Li, Z. Lin, Z. Qian, and J. Wu, "Active DC Bus Signaling Control Method for Coordinating Multiple Energy Storage Devices in DC Microgrid," in *Proc. IEEE Second International Conference on DC Microgrids (ICDCM)*, 2017, pp. 221–226.

[31] Q. Shafiee, T. Dragicevic, J. C. Vasquez, and J. M. Guerrero, "Hierarchical Control for Multiple DC-Microgrids Clusters," *IEEE Trans. Energy Convers.*, vol. 29, no. 4, pp. 922–933, 2014.

[32] L. Zhang, T. Wu, Y. Xing, K. Sun, and J. M. Gurrero, "Power Control of DC Microgrid Using DC Bus Signaling," in *in Proc. IEEE APEC*, 2011, pp. 1926–1932.


Pre-Print

[33] T. Dragicevic, J. M. Guerrero, and J. C. Vasquez, "A Distributed Control Strategy for Coordination of an Autonomous LVDC Microgrid Based on Power-Line Signaling," *IEEE Trans. Ind. Electron.*, vol. 61, no. 7, pp. 3313–3326, Jul. 2014.
[34] D. Boroyevich, I. Cvetkovic, R. Burgos, and D. Dong, "Intergrid: A Future Electronic Energy Network?," *IEEE J. Emerg. Sel. Top. Power Electron.*, vol. 1, no. 3, pp. 127–138, 2013.

Pre Print